

Abstract

The MOZAIC Capacitive Hygrometer (MCH) is usually operated onboard of passenger aircraft in the framework of MOZAIC (Measurement of Ozone by AIRBUS In-Service Aircraft). In order to evaluate the performance of the MCH, it was operated aboard a Learjet 35A aircraft as part of the CIRRUS-III field study together with a closed-cell Lyman- α fluorescence hygrometer (FISH) and an open path tunable diode laser system (OJSTER) for water vapour measurement. After reducing the data set to MOZAIC-relevant conditions, the 1 Hz relative humidity (RH) cross correlation between MCH and reference instruments FISH (clear sky) and OJSTER (in-cirrus) yielded a remarkably good agreement of $R^2 = 0.97$ and slope $m = 0.96$ and provided the MCH uncertainty of 5% RH. Probability distribution functions of RH deduced from MCH and reference instruments agreed well over the entire range of observations. The main limitation for the use of MCH data is related to sensor temperatures below the calibration limit of $T_{\text{sensor}} = -40^\circ\text{C}$ (corresponds to ambient temperature of $T_{\text{ambient}} = -70^\circ\text{C}$ at typical cruising speed of long-haul passenger aircraft), which causes a delay in the sensor's time response. Good performance of MCH for clear sky as well as for in-cirrus conditions demonstrated the sensor robustness also for operation inside ice clouds.

1 Introduction

Water vapour is one of the most important variables for weather prediction and climate research. Particularly, the interaction between the water vapour in the UT/LS (upper troposphere and lowermost stratosphere) and tropopause dynamics is not well understood. Thus, in the latest IPCC report (Stocker et al., 2013), it is stated that the knowledge about potential trends and climate feedback mechanisms of upper tropospheric water vapour is low because of the lack of long data records of high quality in this specific region of the global atmosphere. Neither the global radiosondes network nor satellites can provide measurements of the required spatial and temporal resolution,

AMTD

7, 9803–9838, 2014

Evaluation of MOZAIC Capacitive Hygrometer

P. Neis et al.

Title Page

Abstract

Introduction

Conclusions

References

Tables

Figures



Back

Close

Full Screen / Esc

Printer-friendly Version

Interactive Discussion



The right angle of the minor flow protects the RH and T sensors against dust, water drops, and ice particles.

Due to the strong speed reduction in the inlet part of the housing, the sampled air flow is significantly heated through adiabatic heating. Assuming 100 % conversion of kinetic energy to heat during flow deceleration, the ambient temperature T_{ambient} (Static Air Temperature SAT; see Helten et al., 1998) increases to the temperature at the sensor inside the housing, i.e. the sensor temperature T_{sensor} (Total Air Temperature TAT; see Helten et al., 1998). The relationship between ambient temperature T_{ambient} and sensor temperature T_{sensor} is a function of the aircraft speed, i.e. its Mach-number M :

$$T_{\text{sensor}} = T_{\text{ambient}} \cdot \left(1 + \left(\frac{c_p - c_v}{2c_v} \right) \cdot M^2 \right) \quad (1)$$

where c_p ($= 1005 \text{ J kg}^{-1} \text{ K}^{-1}$) and c_v ($= 717 \text{ J kg}^{-1} \text{ K}^{-1}$) are the specific heat of dry air at constant pressure and volume, respectively. The resulting difference between T_{sensor} and T_{ambient} at 10–12 km cruising altitude for different Mach-numbers is displayed in Fig. 2: for the MOZAIC-typical aircraft speed of $M = 0.81$ the adiabatic heating effect is approx. 30 K. T_{ambient} is derived from Eq. (1) with an uncertainty of less than $\pm 0.5 \text{ K}$ resulting from uncertainties in T_{sensor} ($\pm 0.25 \text{ K}$) and M (Helten et al., 1998). Because of the strong temperature increase, the detected dynamic relative humidity $\text{RH}_{\text{dynamic}}$ (RH_D ; Helten et al., 1998) is significantly lower than the static relative humidity $\text{RH}_{\text{static}}$ (RH_S ; Helten et al., 1998) of the ambient air at T_{ambient} (Helten et al., 1998):

$$\text{RH}_{\text{static}} = \text{RH}_{\text{dynamic}} \cdot \left(\frac{T_{\text{ambient}}}{T_{\text{sensor}}} \right)^{\frac{c_p}{c_p - c_v}} \frac{e_{\text{s, liquid}}(T_{\text{sensor}})}{e_{\text{s, liquid}}(T_{\text{ambient}})} \quad (2)$$

where $e_{\text{s, liquid}}$ is the water vapour saturation pressure over liquid water at T_{sensor} and T_{ambient} , respectively. The water vapour saturation pressure over liquid water $e_{\text{s, liquid}}$ follows the Goff and Gratch (1946) formulation of saturation water vapour pressure over a plane surface of pure water or ice, which was recommended by the World

Evaluation of
MOZAIC Capactive
Hygrometer

P. Neis et al.

Title Page

Abstract

Introduction

Conclusions

References

Tables

Figures



Back

Close

Full Screen / Esc

Printer-friendly Version

Interactive Discussion



Evaluation of MOZAIC Capactive Hygrometer

P. Neis et al.

Title Page

Abstract

Introduction

Conclusions

References

Tables

Figures



Back

Close

Full Screen / Esc

Printer-friendly Version

Interactive Discussion



Meteorological Organization (WMO, 1990) and adapted to their international temperature scale 1990 (ITS-90) by Sonntag (1994). For fast high-flying aircraft the relation $RH_{\text{static}}/RH_{\text{dynamic}}$ reaches a factor of approx. 13 (Helten et al., 1998), which leads to the fact, that the RH sensor operates in the lowest 10 % of its full dynamic range. Since the sensor is operating in the lower part of its full dynamic range, an individual calibration of each sensor is necessary, which is accomplished in the atmospheric simulation chamber at Jülich (Smit et al., 2000) before installation on the aircraft and after detachment past 500 h of flight. These calibrations are made over a sensor temperature range between -40 and $+20^{\circ}\text{C}$ against (i) Lyman- α fluorescence hygrometer (Kley and Stone, 1978) at water vapour mixing ratios below 1000 ppmv (relative accuracy $\pm 4\%$, Helten et al., 1998) and (ii) dew/frost point hygrometer (General Eastern, Type D1311R) at water vapour mixing ratios above 1000 ppmv with an accuracy of $\pm 0.5\text{K}$. The relative humidity of a calibrated sensor (RH_C) at constant temperature T is found to be linearly related to the uncorrected output value (RH_{UC}) provided by the HMP230 transmitter unit (Helten et al., 1998)

$$RH_C(T) = a(T) + b(T) \cdot RH_{UC}(T) \quad (3)$$

Evaluation of 5 years of pre- and post-flight calibrations in MOZAIC has shown that the offset $a(T)$ is the most critical parameter in determining the uncertainty of the measurements, while the sensitivity is less critical and more stable (Smit et al., 2008).

In Sect. 3.2 the calibration procedure of the MCH is described, which was used during the CIRRUS-III field study. It combines the standard procedure based on Helten et al. (1998) and the in-flight calibration described by Smit et al. (2008).

**Evaluation of
MOZAIC Capactive
Hygrometer**

P. Neis et al.

Title Page

Abstract

Introduction

Conclusions

References

Tables

Figures



Back

Close

Full Screen / Esc

Printer-friendly Version

Interactive Discussion



included a MCH and an open path tunable diode laser system (OJSTER; MayComm Instruments, May and Webster, 1993; Krämer et al., 2009) to measure gas phase water vapour VMR. Simultaneously, total water VMR (= gas phase plus ice water) was measured by the reference measurement instrument FISH (Fast In-Situ Hygrometer, Zöger et al., 1999). The closed-cell Lyman- α fluorescence hygrometer was equipped with a forward facing inlet to sample gas phase water in clear sky and total water inside cirrus clouds. To determine whether a data point is in a cirrus cloud or not, the ratio of RH_{ice} from FISH (total water) and OJSTER (water vapour) was used (see Krämer et al., 2009). FISH was calibrated using a laboratory calibration facility with the capability to simulate realistic atmospheric conditions, i.e. water vapour VMR from several hundred to a few ppmv and pressure from 1000 to 10 hPa. Finally, the water vapour mixing ratio was determined using a commercial dew point hygrometer (MBW DP30). The instruments and the parameters derived from their measurements are listed in Table 2.

Prior to the CIRRUS-III campaign the MCH has been (pre-flight) calibrated in the simulation chamber at Forschungszentrum Jülich following the procedures briefly described in chapter 2. Unfortunately a post-flight calibration was not possible due to sensor failure after de-installation of the MCH from the Learjet aircraft at the end of the campaign. From long term experiences of MOZAIC pre- and post-flight calibrations it is well known that over the three months period between the pre-flight calibration and the end of the campaign the offset $a(T)$ can change significantly while the sensitivity $b(T)$ is almost stable over time (see Eq. (3) and Smit et al., 2008). In order to determine the potential drift of the offset $a(T)$ between pre-flight calibration and the end of the campaign the so called in-flight calibration (IFC) method (Smit et al., 2008) has been applied.

Thereby, the sensor offset $a(T)$ at relative humidity below the MCH detection limit has been determined from the measurements themselves as obtained during periods when the aircraft is flying in the lower stratosphere, where the water vapour mixing ratio reached well defined minimum values. In our case, the minimum value in

stratospherically influenced air masses was about 20 ± 1 ppmv as measured by the FISH instrument. Its resulting contribution to the RH_{liquid} -signal of the MCH is minimal. Compared to the pre-flight calibration an offset drift of $(4.5 \pm 1) \% RH_{\text{liquid}}$ was found. The RH_{liquid} -flight data of the MCH obtained during the CIRRUS-III campaign have been corrected for this offset drift. The resulting overall uncertainty of the RH measurements by the MCH, including contributions from temperature uncertainties, is about $\pm 5 \% RH_{\text{liquid}}$ which is in good agreement with the mean uncertainty range obtained from long term MOZAIC-measurements (Smit et al., 2014).

4 Results

4.1 Case study – flight 2

The instrumentation deployed in CIRRUS-III allows an in-flight intercomparison of all water vapour instruments. Figure 4 illustrates an example of the kind of data collected during one research flight on 28 November 2006 (Flight 2). Data from the water vapour sensing instruments used for the intercomparison are shown as VMR. The ambient temperatures T_{ambient} encountered during the flight ranged from -44.1°C to -62.4°C for relevant measurement altitudes. Respective water vapour VMR covered the range from 17 ppmv at the tropopause to approx. 150 ppmv in the free troposphere and even higher values during ascent from and descent into the airport.

For the instrument intercomparison we analysed the sensors with respect to RH_{liquid} since this is the parameter the MCH is calibrated against in the sensor temperature range (see Sect. 2). Further, data for water vapour VMR > 1000 ppmv were excluded in this study because the FISH instrument becomes optically thick and thus insensitive at these conditions (Zöger et al., 1999).

In Fig. 5, we compare RH_{liquid} data and VMR data from MCH (red line) and gas-phase reference (blue line), i.e. OJSTER data in cloud, otherwise FISH data for a complete validation of the MCH for Flight 2. The ambient temperature T_{ambient} (green line) as

Evaluation of MOZAIC Capactive Hygrometer

P. Neis et al.

Title Page

Abstract

Introduction

Conclusions

References

Tables

Figures



Back

Close

Full Screen / Esc

Printer-friendly Version

Interactive Discussion



Evaluation of MOZAIC Capactive Hygrometer

P. Neis et al.

Title Page

Abstract

Introduction

Conclusions

References

Tables

Figures



Back

Close

Full Screen / Esc

Printer-friendly Version

Interactive Discussion



well as the sensor temperature T_{sensor} (black line) measured at the MCH inside the Rosemount housing are shown in the bottom panel. Largest deviations of the MCH to the reference (see e.g. $\Delta\text{RH}_{\text{liquid}}$ in the top panel) are found in clear sky air masses for cold conditions with sensor temperature $T_{\text{sensor}} < -40^\circ\text{C}$ (this corresponds to ambient temperature below approx. -60°C at $M = 0.70$). Except for these extreme conditions, the difference between the MCH and the reference is of the order of 10 % $\text{RH}_{\text{liquid}}$ or less. It has to be noted that regular operation conditions of the MCH aboard long-haul passenger aircraft like A340-300 with a cruising speed of approx. $M = 0.81$ are characterised by sensor temperature $T_{\text{sensor}} \geq -35^\circ\text{C}$ (Helten et al., 1998), whereas during the operation aboard the slower flying Learjet 35A (cruising speed $< M = 0.70$) sensor temperature T_{sensor} values $\leq -40^\circ\text{C}$ were reached since ΔT increases with M (see Fig. 2). Given the fact that during CIRRUS-III the MCH was operated at its lower limit of performance, the agreement with the research-grade reference instruments is remarkably good.

4.2 Assessment of sensor characteristics

4.2.1 Evaluation against reference

In order to prepare a data set for evaluation, data with sensor temperatures $T_{\text{sensor}} < -40^\circ\text{C}$ were excluded because of too dry measurement conditions which were below the MCH calibration limits (see Sect. 2). This fact is illustrated in Fig. 6 showing the difference in $\text{RH}_{\text{liquid}}$ between MCH and reference instruments, i.e. OJSTER data in cloud, otherwise FISH data, according to sensor temperature T_{sensor} . A first overall good agreement of the two sensors down to the calibration limit of -40°C can be stated in the range of $\pm 5\%$. Furthermore, the maximum ambient temperature T_{ambient} was set to the level of instantaneous freezing of -40°C in order to neglect effects of warmer clouds.

Finally, flight sequences of the Learjet 35A with steep ascents and descents were excluded, since these flight conditions are not comparable to conditions aboard long-haul

220 hPa a measured $RH_{\text{liquid}} = 5\%$ with an uncertainty of 5% RH_{liquid} corresponds to a VMR of approx. $5 \text{ ppmv} \pm 5 \text{ ppmv}$.

The proof of validity of the MCH RH_{liquid} data is shown in Fig. 10. As is shown in the bottom panel, the probability distribution function (PDF) for RH_{liquid} derived from MCH data agree very well with those derived from the reference for the entire data set. Larger deviations at higher values of RH_{liquid} , e.g. at possible cirrus cloud edges reflect the fact that the reference instrument FISH measures total water and the data are not classified as cirrus cloud by the algorithm of Krämer et al. (2009). The sensor behaviour for those conditions at the limit of the sensor operation specifications is analysed in detail in the following section.

4.2.2 Sensor characteristics at the limit of its operation range

The comparison between the MCH RH_{liquid} data and the reference RH_{liquid} data, i.e. OJSTER data in cloud, otherwise FISH data, during the CIRRUS-III field study shows a remarkably good agreement for the reduced data set. However, the performance of the MCH sensor in conditions at its limits of operation, e.g. next to the lower calibration limit of $T_{\text{sensor}} = -40^\circ\text{C}$ or during strong humidity changes has to be analysed in detail in order to assess the sensor's operation range. For this purpose, the time series of Flight 2 is revisited in Fig. 11, where the individual RH_{liquid} time series are given in the upper panel, the 60 s moving average of the difference of both RH_{liquid} time series in the middle panel, as well as the T_{sensor} time series in the bottom panel.

The following 3 phases of interest have to be analysed:

- Phase 1 is shaded in blue colour illustrates a strong humidity change while flying through a cirrus cloud. Because of slower MCH sensor response at colder sensor temperatures, the MCH RH_{liquid} values (green line) can not follow the rapid changes in RH_{liquid} as observed by the reference (blue line). However, as was shown previously in Fig. 10, there is no statistically significant effect of the delayed sensor response to strong humidity changes at low temperatures.

Evaluation of MOZAIC Capactive Hygrometer

P. Neis et al.

Title Page

Abstract

Introduction

Conclusions

References

Tables

Figures



Back

Close

Full Screen / Esc

Printer-friendly Version

Interactive Discussion



Evaluation of MOZAIC Capactive Hygrometer

P. Neis et al.

- Phase 2 is shaded in red and refers to a section of the flight when T_{sensor} reaches values below the sensor calibration limit of $T_{\text{sensor}} = -40^{\circ}\text{C}$, i.e. ambient temperatures below -70°C at commercial aircraft speed of Mach-number $M = 0.81$. The MCH shows reduced performance and increasing deviations between the MCH and the reference instruments occur.
- Phase 3 shaded in grey refers to mixed conditions with isolated rapid humidity changes, while flying through small cirrus clouds those rapid $\text{RH}_{\text{liquid}}$ changes are superimposed by strong temperature changes because of the aircraft ascent to measurement altitude and the occurrence of temperatures below the calibration limit, which both cause a reduction of the MCH time resolution.

Despite of reduced sensor response to conditions at the limit of its operation range, the MCH shows a very good overall performance during the CIRRUS-III field study. Figure 12 compares frequency of occurrence (top panel) and PDF (bottom panel) of $\text{RH}_{\text{liquid}}$ based on 5 % $\text{RH}_{\text{liquid}}$ bins of the complete MCH data set, i.e. all data points above the homogenous freezing threshold of $T_{\text{ambient}} = -40^{\circ}\text{C}$, with those of the data set reduced to MOZAIC-relevant conditions. The comparison of the observed $\text{RH}_{\text{liquid}}$ counts and PDF per 5 % bin demonstrates the equivalence of the statistical distribution of $\text{RH}_{\text{liquid}}$ of both data sets. Main quantitative deviations are observed in the transition region between clear sky ($< 25\% \text{RH}_{\text{liquid}}$) and next to cirrus clouds ($> 50\% \text{RH}_{\text{liquid}}$) during rapid changes in flight altitude at very cold conditions and therefore with a longer sensor response time at flight sequences into and out of cirrus clouds.

Figure 13 shows the PDF of water vapour VMR data as a function of T_{ambient} (panels a–c for the complete data set and panels d–f for the reduced data set, respectively) according to Kunz et al. (2008). The frequencies of occurrence are calculated in 1°C bins for the MCH data set (panels a and d), the reference data set (panels b and e) and the deviation of both PDF's (panel c and f). The water vapour VMR is binned logarithmically spaced between 0 and 8.0 with a bin size of 0.8. The colour bars are binned in 5 % spaces for a better interpretation of the contour plots.

Title Page

Abstract

Introduction

Conclusions

References

Tables

Figures



Back

Close

Full Screen / Esc

Printer-friendly Version

Interactive Discussion



The MCH seems to remain at dryer values for the coldest temperatures of $T_{\text{ambient}} \cong -60^{\circ}\text{C}$, which is again a result of the delayed sensor response at sensor temperatures below the calibration limit. Further, small deviations at lower temperatures are also observed. In summary data sets for both cases show a similar behaviour in the water vapour VMR distribution with only small deviations but as shown before in Fig. 12 these deviations have no statistically significant relevance.

5 Conclusions and recommendations

The CIRRUS-III (2006) aircraft campaign provided a data set for evaluating the MOZAIC Capacitive Hygrometer (MCH) in a blind intercomparison with high performance water vapour instruments based on tunable diode laser absorption spectrometry (in-cloud reference) and Lyman- α fluorescence detection (clear sky reference).

Except for conditions at its operation limit (e.g., at sensor temperatures $T_{\text{sensor}} < -40^{\circ}\text{C}$ and during rapid changes in $\text{RH}_{\text{liquid}}$), the MCH performs with a difference of 10% $\text{RH}_{\text{liquid}}$ or less to the references, i.e. OJSTER data in cloud, otherwise FISH data.

In order to obtain a representative result for the MCH's uncertainty for its regular deployment aboard passenger aircraft, the data set was restricted to more MOZAIC relevant conditions: data with sensor temperatures below -40°C were excluded due to the calibration limit. In MOZAIC less than 1% of RH observations are made at sensor temperatures colder than -40°C . Strong ascent and descent sequences of the aircraft were removed and the maximum ambient temperature (T_{ambient}) was set to -40°C to exclude effects of warm clouds.

The 1 Hz correlation yielded a robust linear fit with a slope of unity, with no statistically significant offset and a correlation coefficient of $R^2 = 0.92$ which was confirmed by the correlation of the binned $\text{RH}_{\text{liquid}}$ data. The $\text{RH}_{\text{liquid}}$ data grouped in 5% $\text{RH}_{\text{liquid}}$ bins agree very well for the MCH and reference instruments over the entire cloud-free range and for most of the cirrus clouds sequences and yield MCH uncertainty of 5% $\text{RH}_{\text{liquid}}$.

Evaluation of MOZAIC Capacitive Hygrometer

P. Neis et al.

Title Page

Abstract

Introduction

Conclusions

References

Tables

Figures



Back

Close

Full Screen / Esc

Printer-friendly Version

Interactive Discussion



Evaluation of MOZAIC Capactive Hygrometer

P. Neis et al.

Title Page

Abstract

Introduction

Conclusions

References

Tables

Figures



Back

Close

Full Screen / Esc

Printer-friendly Version

Interactive Discussion



Comparing the MCH's and references' probability distribution functions (PDF) for RH_{liquid} shows no statistically significant effect of delayed sensor response because of the limitations of the MCH. Neither strong humidity changes, nor operation at the lower calibration limits causes considerable sensor failures. The main limitation for the use of MCH RH_{liquid} data are related to sensor temperatures below the calibration limit of $T_{\text{sensor}} = -40^{\circ}\text{C}$. However, these temperatures are encountered only infrequently in the MOZAIC programme as long as the current flight tracks don't reach polar air masses with ambient temperatures below -70°C . In summary, the MCH is highly suitable for climatology analyses in the MOZAIC programme even if the sensor is not applicable to high time resolution measurements.

A value for the limit of detection is not appropriate for the MCH, but the variable to describe its performance is the here determined uncertainty of the RH_{liquid} measurements. RH_{liquid} measurements below 5 %, which are common in the lowermost stratosphere, have to be used carefully because these data are close to the sensor uncertainty range, which as shown before in Sect. 4.2.1, results in a relative deviation of 100 %.

Acknowledgements. The authors gratefully acknowledge Peter Spichtinger (Mainz Univ.) for fruitful discussions. The support by *enviscope* GmbH at the technical organization of the field study is also appreciated. Part of this work was funded by the German Federal Ministry for Research and Education (BMBF) in the framework of the joint programme IAGOS-D under Grant No. 01LK1223A.

The service charges for this open access publication have been covered by a Research Centre of the Helmholtz Association.

References

- Bange, J., Esposito, M., Lenschow, D. H., Brown, P. R. A., Dreiling, V., Giez, A., Mahrt, L., Malinowski, S. P., Rodi, A. R., Shaw, R. A., Siebert, H., Smit, H., and Zöger, M.: Measurement of Aircraft State and Thermodynamic and Dynamic Variables, in: Airborne Measurements for Environmental Research: Methods and Instruments, edited by: Wendisch, M. and Brenguier, J.-L., Wiley-VCH Verlag GmbH & Co. KGaA, Weinheim, Germany, doi:10.1002/9783527653218.ch2, 2013. 9823
- 5 Gierens, K., Schumann, U., Smit, H., Helten, M., and Zangl, G.: Determination of humidity and temperature fluctuations based on MOZAIC data and parametrisation of persistent contrail coverage for general circulation models, *Ann. Geophys.*, 15, 1057–1066, doi:10.1007/s00585-997-1057-3, 1997. 9805
- 10 Gierens, K., Schumann, U., Helten, M., Smit, H., and Marenco, A.: A distribution law for relative humidity in the upper troposphere and lower stratosphere derived from three years of MOZAIC measurements, *Ann. Geophys.*, 17, 1218–1226, doi:10.1007/s00585-999-1218-7, 1999. 9805
- 15 Gierens, K., Schumann, U., Helten, M., Smit, H., and Wang, P.: Ice-supersaturated regions and subvisible cirrus in the northern midlatitude upper troposphere, *J. Geophys. Res.-Atmos.*, 105, 22743–22753, doi:10.1029/2000JD900341, 2000. 9805
- 20 Goff, J. A. and Gratch, S.: Low-pressure properties of water from -160 to 212 F, *Trans. Amer. Soc. Heat. Vent. Eng.*, 51, 125–164, 1946. 9807
- Helten, M., Smit, H., Strater, W., Kley, D., Nedelec, P., Zoger, M., and Busen, R.: Calibration and performance of automatic compact instrumentation for the measurement of relative humidity from passenger aircraft, *J. Geophys. Res.-Atmos.*, 103, 25643–25652, doi:10.1029/98JD00536, International Workshop on Biogenic Hydrocarbons in the Atmospheric Boundary Layer, Univ. Virginia, Charlottesville, VA, August 1997, 1998. 9805, 9807, 25 9808, 9812, 9823, 9826, 9827
- Helten, M., Smit, H., Kley, D., Ovarlez, J., Schlager, H., Baumann, R., Schumann, U., Nedelec, P., and Marenco, A.: In-flight comparison of MOZAIC and POLINAT water vapor measurements, *J. Geophys. Res.-Atmos.*, 104, 26087–26096, doi:10.1029/1999JD900315, 30 1999. 9805, 9806, 9809, 9813

Evaluation of MOZAIC Capacitive Hygrometer

P. Neis et al.

Title Page

Abstract

Introduction

Conclusions

References

Tables

Figures



Back

Close

Full Screen / Esc

Printer-friendly Version

Interactive Discussion



Evaluation of MOZAIC Capacitive Hygrometer

P. Neis et al.

Title Page

Abstract

Introduction

Conclusions

References

Tables

Figures



Back

Close

Full Screen / Esc

Printer-friendly Version

Interactive Discussion



- Kley, D. and Stone, E.: Measurement of water-vapor in stratosphere by photo-dissociation with ly-alpha-(1216 A) light, *Rev. Sci. Instrum.*, 49, 691–697, doi:10.1063/1.1135596, 1978. 9808
- Kley, D., Smit, H. G. J., Nawrath, S., Luo, Z., Nedelec, P., and Johnson, R. H.: Tropical Atlantic convection as revealed by ozone and relative humidity measurements, *J. Geophys. Res.-Atmos.*, 112, D23109, doi:10.1029/2007JD008599, 2007. 9805
- Krämer, M., Schiller, C., Afchine, A., Bauer, R., Gensch, I., Mangold, A., Schlicht, S., Spelten, N., Sitnikov, N., Borrmann, S., de Reus, M., and Spichtinger, P.: Ice supersaturations and cirrus cloud crystal numbers, *Atmos. Chem. Phys.*, 9, 3505–3522, doi:10.5194/acp-9-3505-2009, 2009. 9810, 9814
- Kunz, A., Schiller, C., Rohrer, F., Smit, H. G. J., Nedelec, P., and Spelten, N.: Statistical analysis of water vapour and ozone in the UT/LS observed during SPURT and MOZAIC, *Atmos. Chem. Phys.*, 8, 6603–6615, doi:10.5194/acp-8-6603-2008, 2008. 9815
- Luo, Z., Kley, D., Johnson, R. H., and Smit, H.: Ten years of measurements of tropical upper-tropospheric water vapor by MOZAIC. Part I: Climatology, variability, transport, and relation to deep convection, *J. Climate*, 20, 418–435, doi:10.1175/JCLI3997.1, 2007. 9805
- Luo, Z., Kley, D., Johnson, R. H., and Smit, H.: Ten years of measurements of tropical upper-tropospheric water vapor by MOZAIC. Part II: Assessing the ECMWF humidity analysis, *J. Climate*, 21, 1449–1466, doi:10.1175/2007JCLI1887.1, 2008. 9805
- Marenco, A., Thouret, V., Nedelec, P., Smit, H., Helten, M., Kley, D., Karcher, F., Simon, P., Law, K., Pyle, J., Poschmann, G., Von Wrede, R., Hume, C., and Cook, T.: Measurement of ozone and water vapor by Airbus in-service aircraft: the MOZAIC airborne program, an overview, *J. Geophys. Res.-Atmos.*, 103, 25631–25642, doi:10.1029/98JD00977, International Workshop on Biogenic Hydrocarbons in the Atmospheric Boundary Layer, Univ. Virginia, Charlottesville, VA, August 1997, 1998. 9805
- May, R. and Webster, C.: Data-processing and calibration for tunable diode-laser harmonic absorption spectrometers, *J. Quant. Spectrosc. Ra.*, 49, 335–347, doi:10.1016/0022-4073(93)90098-3, 1993. 9810, 9823
- Mottaghy, D.: Ozonmessungen in der unteren Stratosphäre, Master's thesis, Rheinisch-Westfälische Technische Hochschule Aachen, in cooperation with the Institute for Chemistry and Dynamics of the Geosphere, ICG-1: Stratosphere, 2001. 9809
- Petzold, A., Volz-Thomas, A., Thouret, V., Cammas, J.-P., and Brenninkmeijer, C.: IAGOS – In-service Aircraft for a Global Observing System, in: 3rd International Conferene on Transport, Atmosphere and Climate, edited by: Sausen, R., Unterstrasser, S., and Blum, A.,

Evaluation of MOZAIC Capacitive Hygrometer

P. Neis et al.

Title Page

Abstract

Introduction

Conclusions

References

Tables

Figures



Back

Close

Full Screen / Esc

Printer-friendly Version

Interactive Discussion



Forschungsbericht 2012-17, Deutsches Zentrum für Luft- und Raumfahrt, Oberpfaffenhofen, Germany, 69–76, 2013. 9805

Schlager, H., Konopka, P., Schulte, P., Schumann, U., Ziereis, H., Arnold, F., Klemm, M., Hagen, D., Whitefield, P., and Ovarlez, J.: In situ observations of air traffic emission signatures in the North Atlantic flight corridor, *J. Geophys. Res.-Atmos.*, 102, 10739–10750, doi:10.1029/96JD03748, 1997. 9805

Schumann, U.: Pollution from aircraft emissions in the North Atlantic flight corridor (POLINAT), vol. *Air Pollut. Res. Rep. 58*, Rep. EUR 16978 EN, Europ. Commission, Luxembourg, 1997. 9805

Smit, H., Sträter, W., Helten, M., and Kley, D.: Environmental Simulation Facility to Calibrate Airborne Ozone and Humidity Sensors, Tech. rep., Report No. 3796, Berichte des Forschungszentrums Jülich, 2000. 9808

Smit, H. G. J., Volz-Thomas, A., Helten, M., Paetz, W., and Kley, D.: An in-flight calibration method for near-real-time humidity measurements with the airborne MOZAIC sensor, *J. Atmos. Ocean. Tech.*, 25, 656–666, doi:10.1175/2007JTECHA975.1, 2008. 9805, 9808, 9810

Smit, H. G. J., Rohs, S., Neis, P., Boulanger, D., Krämer, M., Wahner, A., and Petzold, A.: Technical Note: Reanalysis of upper troposphere humidity data from the MOZAIC programme for the period 1994 to 2009, *Atmos. Chem. Phys. Discuss.*, 14, 18905–18942, doi:10.5194/acpd-14-18905-2014, 2014. 9805, 9811

Sonntag, D.: Advancements in the field of hygrometry, *Meteorol. Z.*, 3, 51–66, 1994. 9808

Spichtinger, P., Gierens, K., Leiterer, U., and Dier, H.: Ice supersaturation in the tropopause region over Lindenberg, Germany, *Meteorol. Z.*, 12, 143–156, doi:10.1127/0941-2948/2003/0012-0143, 2003. 9805

Stickney, T. M., Shedlov, M., and Thompson, D. I.: Rosemount total temperature sensors, Tech. rep., Tech. Rep. 5755, Revision B, Aerosp. Div. Rosemount Inc., 1990. 9806

Stocker, T. F., Qin, D., Plattner, G.-K., Tignor, M., Allen, S. K., Boschung, J., Nauels, A., Xia, Y., Bex, V., and Midgley, P. M.: *Climate change 2013: the Physical Science Basis*, Intergovernmental Panel on Climate Change, Working Group I Contribution to the IPCC Fifth Assessment Report (AR5), Cambridge Univ. Press, New York, 2013. 9804

WMO: World Meteorological Organization: measurement of atmospheric humidity, Tech. rep., in: *Guide to Meteorological Instruments and Methods of Observation*, 5th Edn., WMO Rep. 8, 5.1–5.19, Geneva, 1990. 9808

Zöger, M., Afchine, A., Eicke, N., Gerhards, M., Klein, E., McKenna, D., Morschel, U., Schmidt, U., Tan, V., Tuitjer, F., Woyke, T., and Schiller, C.: Fast in situ stratospheric hygrometers: a new family of balloon-borne and airborne Lyman alpha photofragment fluorescence hygrometers, *J. Geophys. Res.-Atmos.*, 104, 1807–1816, doi:10.1029/1998JD100025, 1999. 9810, 9811, 9823

5

Evaluation of MOZAIC Capacitive Hygrometer

P. Neis et al.

Title Page

Abstract

Introduction

Conclusions

References

Tables

Figures



Back

Close

Full Screen / Esc

Printer-friendly Version

Interactive Discussion



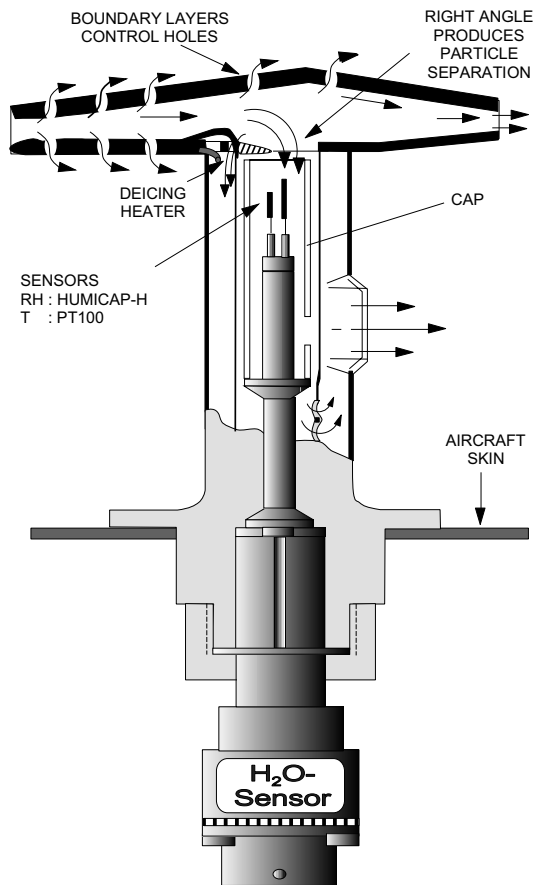


Figure 1. Cross section of the airborne capacitive sensing element. Right angle protects against particles and control holes in the side wall neglect internal boundary layer effects (Helten et al., 1998).

Evaluation of MOZAIC Capacitive Hygrometer

P. Neis et al.

Title Page

Abstract

Introduction

Conclusions

References

Tables

Figures



Back

Close

Full Screen / Esc

Printer-friendly Version

Interactive Discussion



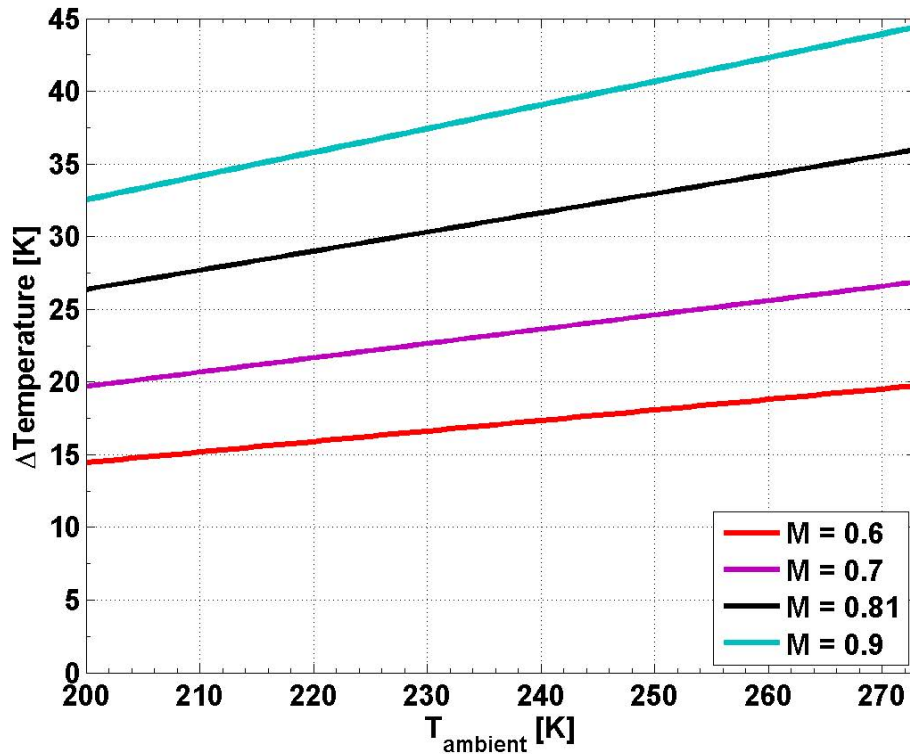


Figure 2. Sampled air flow is heated through adiabatic heating effects when entering the inlet. $\Delta\text{Temperature}$ describes the increase relative to the ambient temperature T_{ambient} (Static Air Temperature SAT; see Helten et al., 1998) for several aircraft speeds, i.e. the Mach-number M , by assuming 100 % conversion of kinetic energy to heat during flow deceleration.

Evaluation of MOZAIC Capacitive Hygrometer

P. Neis et al.

Title Page

Abstract

Introduction

Conclusions

References

Tables

Figures



Back

Close

Full Screen / Esc

Printer-friendly Version

Interactive Discussion



AMTD

7, 9803–9838, 2014

Evaluation of
MOZAIC Capacitive
Hygrometer

P. Neis et al.

Title Page

Abstract

Introduction

Conclusions

References

Tables

Figures



Back

Close

Full Screen / Esc

Printer-friendly Version

Interactive Discussion

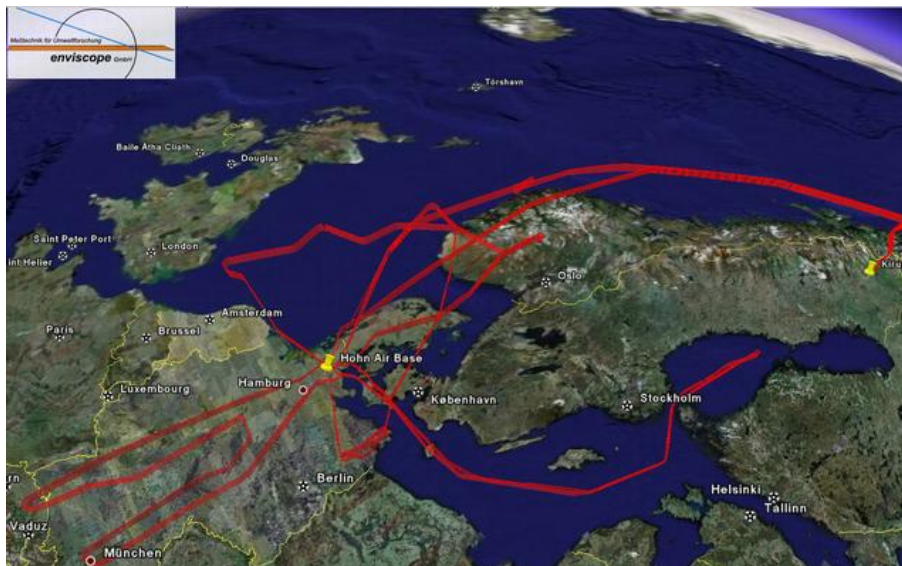


Figure 3. CIRRUS-III flight track overview (Map Data © 2008 Google, Sanborn).

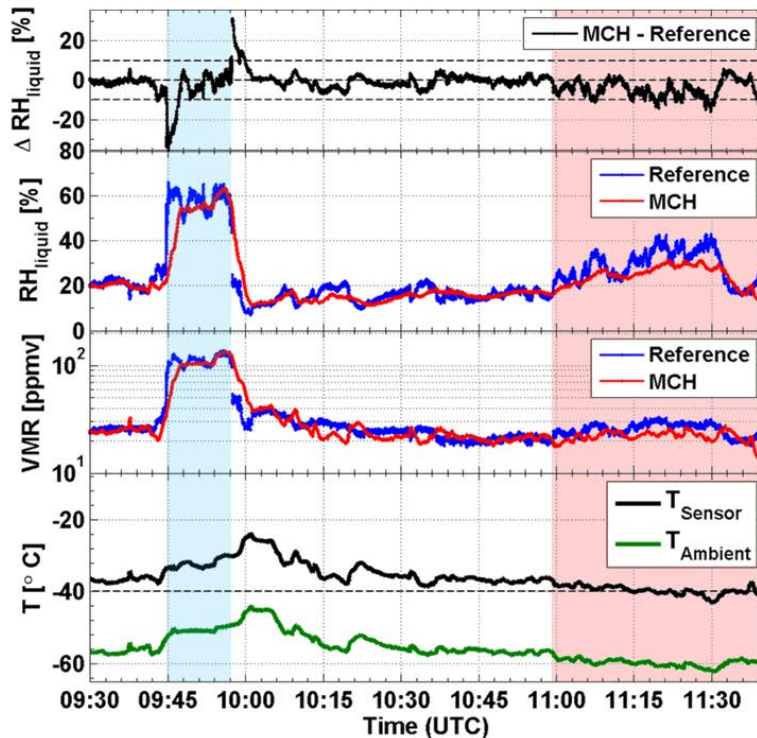


Figure 5. Top-down: $\Delta RH_{\text{liquid}}$ (MCH-reference), RH_{liquid} and VMR measured by the MCH (red) and the reference (blue), i.e. FISH (clear sky) and OJSTER (in-cirrus), as a function of flight time during flight 2 on 28 November 2006. Sensor temperature T_{sensor} (black) as well as ambient temperature T_{ambient} (green) are shown in the bottom panel of the figure. The blue-shaded area represents air masses with high humidity and possible cirrus cloud. Air masses with sensor temperatures at and below the calibration limit are shaded in red.

Evaluation of
MOZAIC Capacitive
Hygrometer

P. Neis et al.

Title Page

Abstract Introduction

Conclusions References

Tables Figures

◀ ▶

◀ ▶

Back Close

Full Screen / Esc

Printer-friendly Version

Interactive Discussion



Evaluation of MOZAIC Capacitive Hygrometer

P. Neis et al.

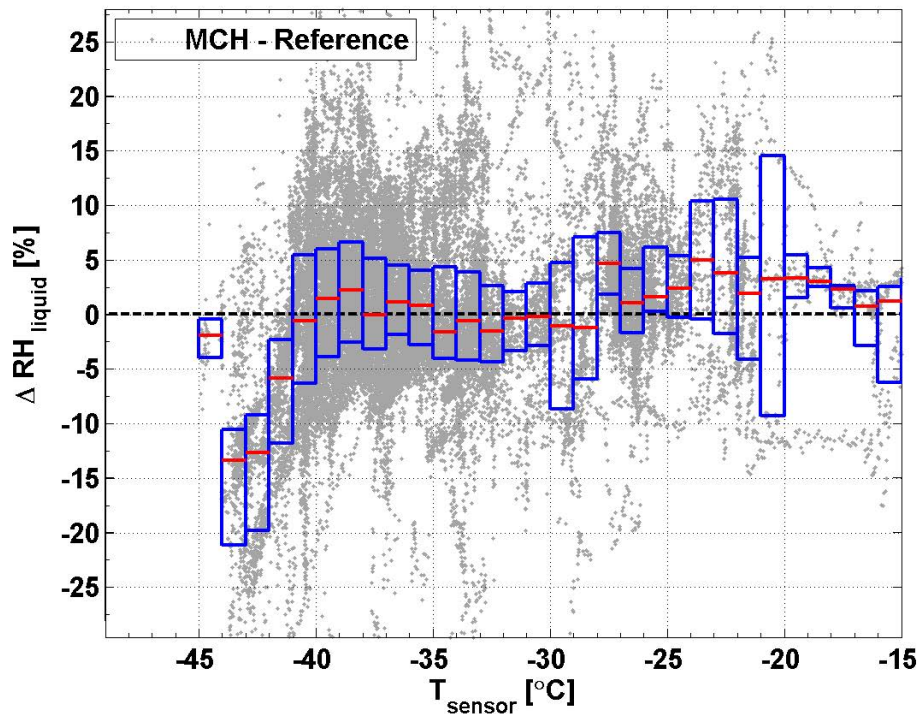


Figure 6. Differences in relative humidity $\text{RH}_{\text{liquid}}$ of MCH and reference, i.e. FISH (clear sky) and OJSTER (in-cirrus), are scattered against the sensor temperature T_{sensor} . A drift towards too dry MCH measurements below the calibration limit of -40°C is clearly seen. The median values (red lines in the box) of the 1°C -binned data as well as the 25th and 75th percentiles are within the calibration limits.

[Title Page](#)[Abstract](#)[Introduction](#)[Conclusions](#)[References](#)[Tables](#)[Figures](#)[◀](#)[▶](#)[◀](#)[▶](#)[Back](#)[Close](#)[Full Screen / Esc](#)[Printer-friendly Version](#)[Interactive Discussion](#)

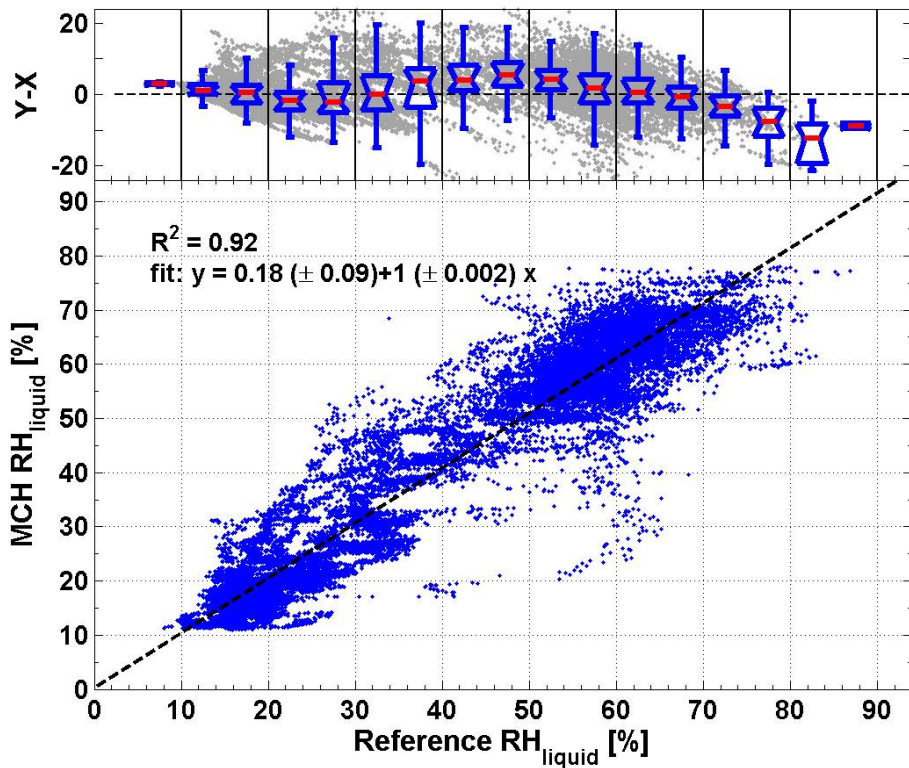


Figure 7. Bottom: Comparison cross plot between reference, i.e. FISH (clear sky) and OJSTER (in-cirrus), and MCH RH_{liquid} displayed as scatter plot with robust fitting curve (dashed line). Top: The related comparison cross plot between the reference and the difference of MCH (y) and reference (x) values is shown again as scatter plot. The additional box-and-whisker-plot represents the median, 25th/75th and outer values for the RH_{liquid} differences per 5% RH_{liquid} bin.

Evaluation of MOZAIC Capacitive Hygrometer

P. Neis et al.

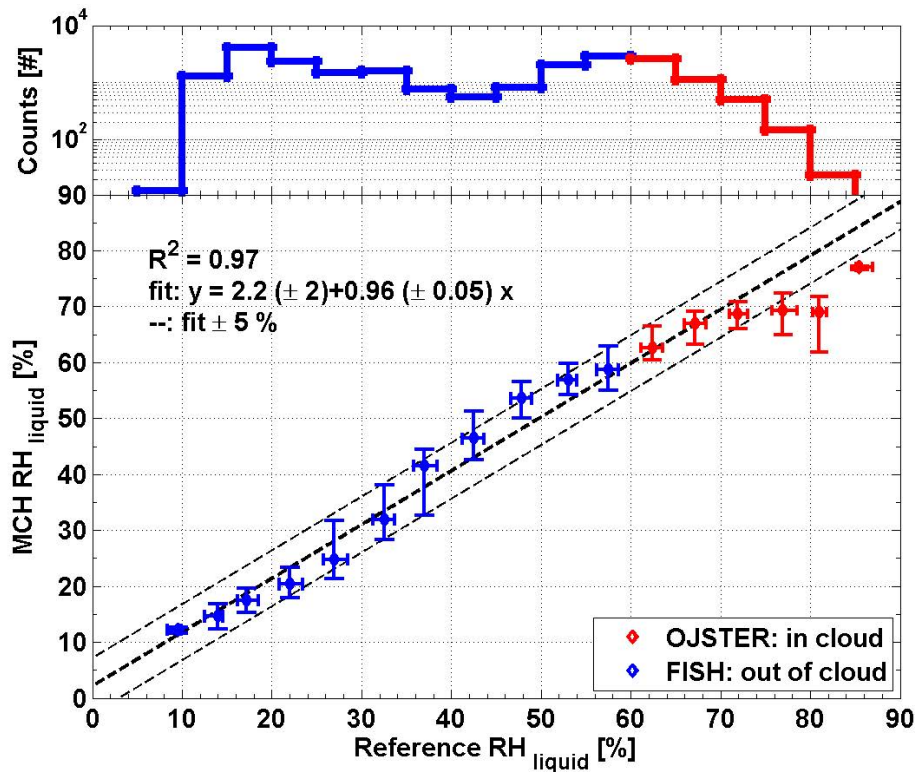


Figure 8. Correlation of $\text{RH}_{\text{liquid}}$ data from MCH and FISH/OJSTER during CIRRUS-III; the straight line indicates the linear regression line while the dashed lines illustrate the sensor uncertainty range $\pm 5\% \text{RH}_{\text{liquid}}$. The top panel shows the number of data points per $5\% \text{RH}_{\text{liquid}}$ bin.

Evaluation of MOZAIC Capacitive Hygrometer

P. Neis et al.

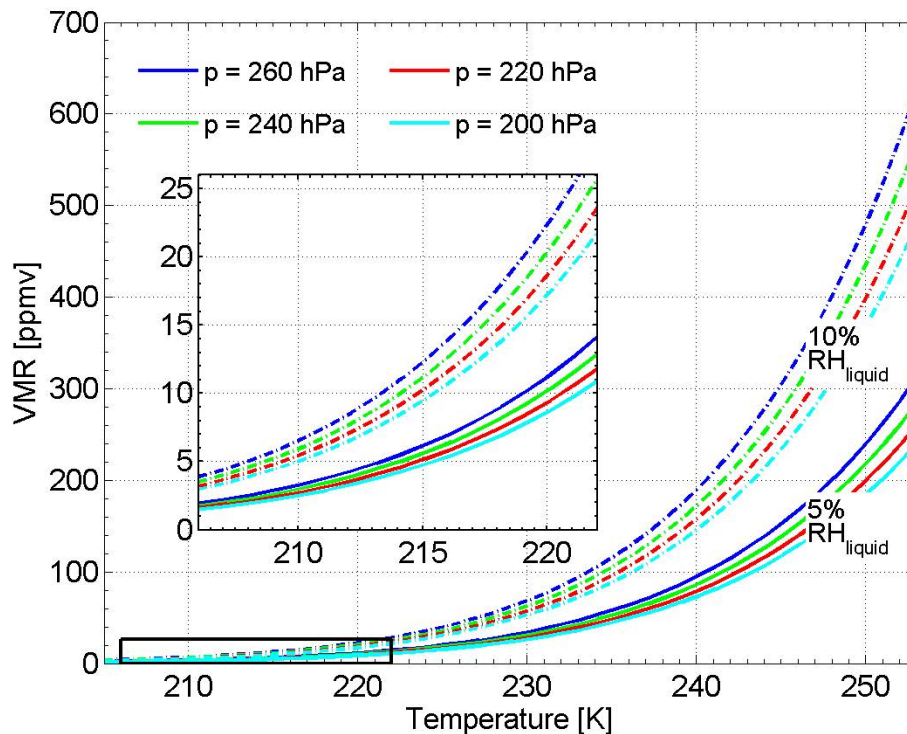


Figure 9. Water vapour volume mixing ratios (VMR) as a function of ambient temperature for 5% (solid lines) and 10% RH_{liquid} (dashed lines), respectively. The different pressure levels represent typical passenger aircraft flight altitudes. The inner box shows a zoom of the lower temperature and VMR values.

Title Page

Abstract

Introduction

Conclusions

References

Tables

Figures

◀

▶

◀

▶

Back

Close

Full Screen / Esc

Printer-friendly Version

Interactive Discussion



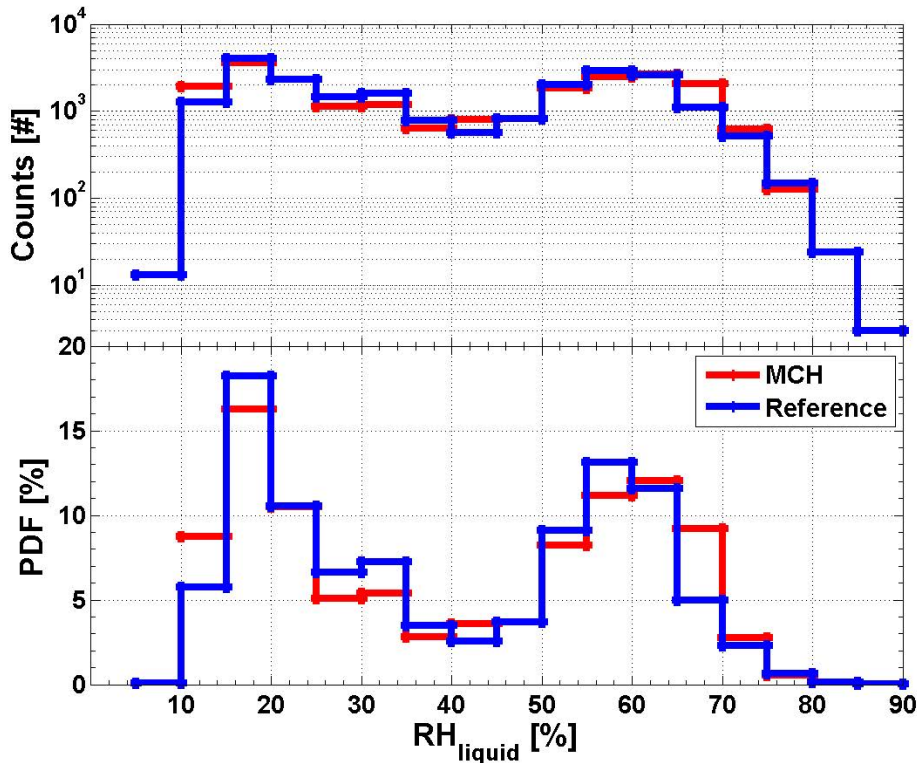


Figure 10. Number of data points (top) and frequency of occurrence (bottom) for observations of RH_{liquid} during CIRRUS III; blue and red lines refer to data from reference, i.e. FISH (clear sky) and OJSTER (in-cirrus), and MCH, respectively. The number of counts of both data sets agree in almost all 5% RH_{liquid} bins. The exponential decline at higher values is in accordance to the result of Spichtinger et al. A bimodal distribution can be seen clearly in the probability density function (PDF) view of the data sets, where there is a clear sky section at lower values and a cirrus section at higher values, respectively. The differences in the PDF distribution can be mainly explained by the longer response time of the MCH into and out of the clouds.

**Evaluation of
MOZAIC Capacitive
Hygrometer**

P. Neis et al.

Title Page

Abstract

Introduction

Conclusions

References

Tables

Figures

◀

▶

◀

▶

Back

Close

Full Screen / Esc

Printer-friendly Version

Interactive Discussion



Evaluation of MOZAIC Capacitive Hygrometer

P. Neis et al.

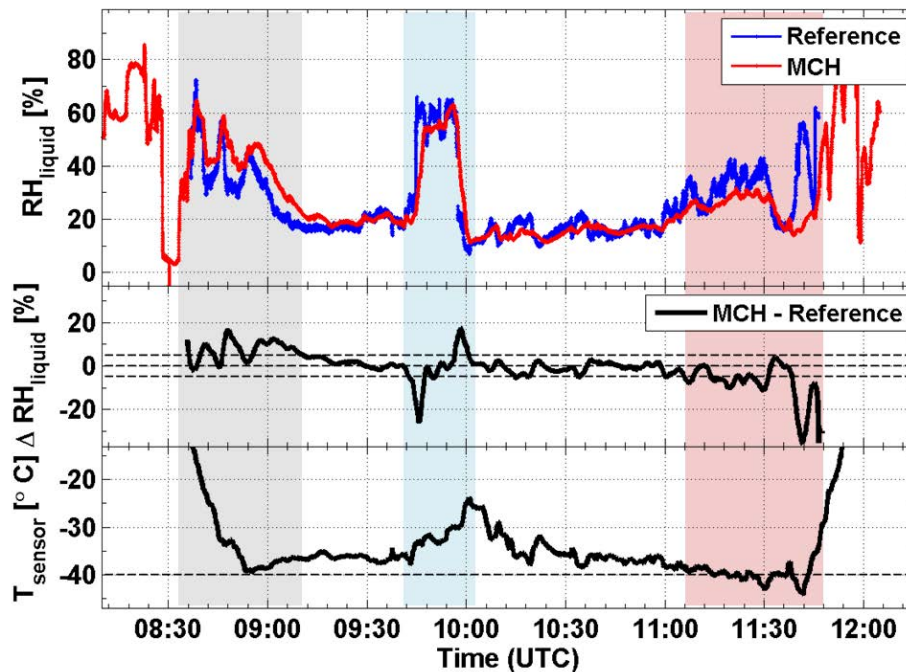


Figure 11. Upper panel shows the RH_{liquid} data from MCH (red) and reference (blue), i.e. FISH (clear sky) and OJSTER (in-cirrus), during CIRRUS-III flight on 28 November 2006. The 60 s moving average of the difference of both RH_{liquid} time series is given in the middle panel. Further, the sensor temperature T_{sensor} time series reaches the lower calibration limit of -40°C several times in the lower panel. The shaded areas represent different limitations for the sensor. Blue: strong humidity change (cirrus cloud), Red: sensor temperature below calibration limit, grey: combination of flying through a small cirrus with steep ascent and very cold sensor temperature, respectively

Title Page

Abstract

Introduction

Conclusions

References

Tables

Figures

◀

▶

◀

▶

Back

Close

Full Screen / Esc

Printer-friendly Version

Interactive Discussion



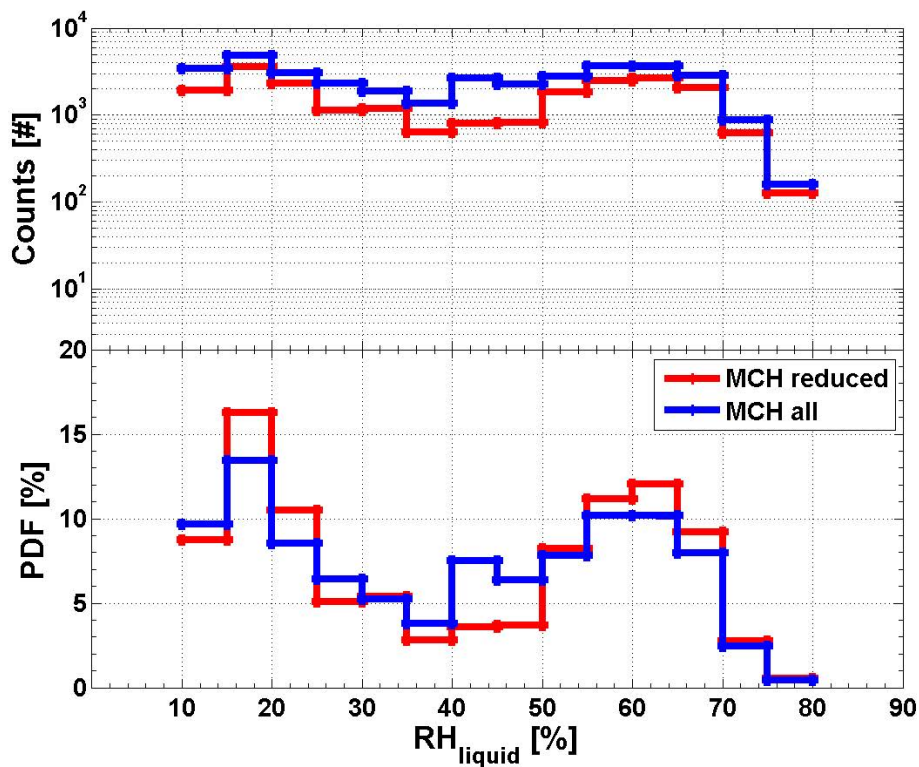


Figure 12. Counts (top) and frequency of occurrence (bottom) for observations of RH_{liquid} during CIRRUS III; blue and red lines refer to data from the complete and reduced MCH data, respectively.

**Evaluation of
MOZAIC Capacitive
Hygrometer**

P. Neis et al.

Title Page

Abstract

Introduction

Conclusions

References

Tables

Figures

◀

▶

◀

▶

Back

Close

Full Screen / Esc

Printer-friendly Version

Interactive Discussion



Evaluation of MOZAIC Capacitive Hygrometer

P. Neis et al.

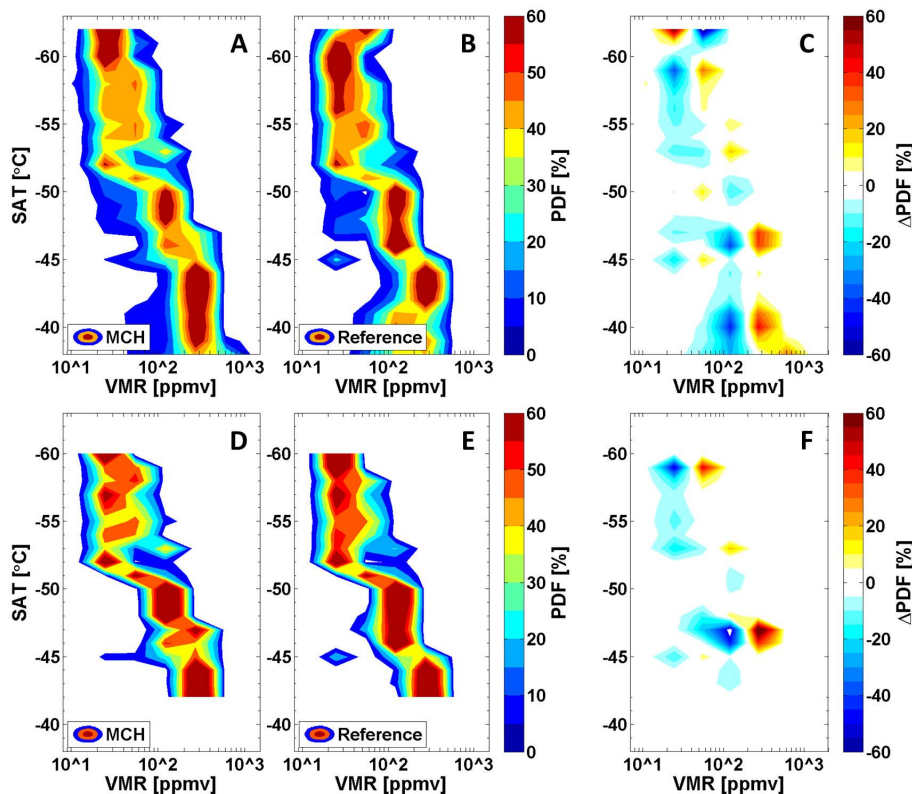


Figure 13. Probability density function (PDF) of the complete (a–c) and reduced (d–f) MCH (a, d) and reference (b, e), i.e. FISH (clear sky) and OJSTER (in-cirrus), water vapour volume mixing ratio (VMR) data related to the ambient temperature T_{ambient} , respectively. Water vapour volume mixing ratio is binned in the logarithmical space between 0 and 8.8 with a bin size of 0.8, the temperature in 1°C bins. Panels (c) and (f) show the difference of the complete and reduced data PDFs.